Available online at www.sciencedirect.com
SCIENCE DIRECT
Journal of Solid State Chemistry 179 (2006) 2281–2289
JOURNAL OF SOLID STATE CHEMISTRY
www.elsevier.com/locate/jssc

Thermal stability of high surface area silicon carbide materials

Piotr Krawiec, Stefan Kaskel*

Department of Inorganic Chemistry, Technical University of Dresden, Mommsenstr. 6, D-01062 Dresden, Germany

Received 2 January 2006; received in revised form 28 February 2006; accepted 28 February 2006
Available online 12 March 2006

Dedicated to Prof. Hans Georg von Schnering for his 75th birthday.

Abstract

The synthesis of mesoporous silicon carbide by chemical vapor infiltration of dimethyl dichlorosilane into mesoporous silica SBA-15 and subsequent dissolution of the silica matrix with HF was investigated. The influence of the synthesis parameters of the composite material (SiC/SBA-15) on the final product (mesoporous SiC) was determined. Depending on the preparation conditions, materials with specific surface areas from 410 to 830 $m^2 g^{-1}$ and pore sizes between 2 and 10 nm with high mesopore volume (0.31–0.96 $cm^3 g^{-1}$) were prepared. Additionally, the thermal stability of mesoporous silicon carbide at 1573 K in an inert atmosphere (argon) was investigated, and compared to that of SBA-15 and ordered mesoporous carbon (CMK-1). Mesoporous SiC has a much higher thermal textural stability as compared to SBA-15, but a lower stability than ordered mesoporous carbon CMK-1.

Keywords: Silicon carbide; High surface area; Mesoporous materials

1. Introduction

Silicon carbide is a material with excellent heat conductivity, hardness and high-temperature mechanical stability [1]. SiC has been widely studied as a dense ceramic [2,3] and has been used for the preparation of composite materials [4,5]. Especially the preparation of nano-sized silicon carbide has received considerable attention, since it allows the preparation of bulk materials with increased plasticity [6] or nano-composites with enhanced mechanical and tribological properties [7]. Due to the chemical inertness it was also proposed to be an interesting catalyst support [8], with unusual high-temperature stability. Although the stability of high surface area silicon carbide under oxidizing conditions at higher temperatures was found to be low due to the passivation of the surface, under inert conditions the material retains a high surface area for longer duration [9]. Several reports were published, showing that this material effectively competes with conventional supports, such as alumina, silica or activated carbons, especially in exothermic reactions where heat conductivity of the support plays a crucial role [10–14].

However, commercially available silicon carbide has a low specific surface area ($S_g < 25\ m^2 g^{-1}$) and is not suitable as a catalyst support. Thus, new methods were developed for the preparation of the high surface area materials. One of the first procedures for the manufacture of carbide materials with surface areas up to 200 $m^2 g^{-1}$ was "shape memory synthesis". High surface area activated carbon was reacted with SiO at elevated temperatures for the synthesis of silicon carbide [10]. On the other hand, reduction of high surface area silica with carbon precursors also leads to high surface area silicon carbide materials. An example is the reduction of high surface area silica aerogels with carbon precursors for the production of materials with a specific surface area of 112 $m^2 g^{-1}$ [15]. The same idea of reacting silicon or silica with carbon can be used to prepare silicon carbide from ordered mesoporous materials, but in this case, surface areas do not exceed 160 $m^2 g^{-1}$ [16–18]. The decomposition of simple silane precursors at low pressures can be used for the manufacture of SiC with a surface area of 50 $m^2 g^{-1}$ [13], or at high autogenic pressures 146 $m^2 g^{-1}$ can be achieved [19]. Chemical vapor

*Corresponding author. Fax: +49 35104633 7287.
E-mail address: Stefan.kaskel@chemie.tu-dresden.de (S. Kaskel).

0022-4596/$ - see front matter © 2006 Elsevier Inc. All rights reserved.
doi:10.1016/j.jssc.2006.02.034

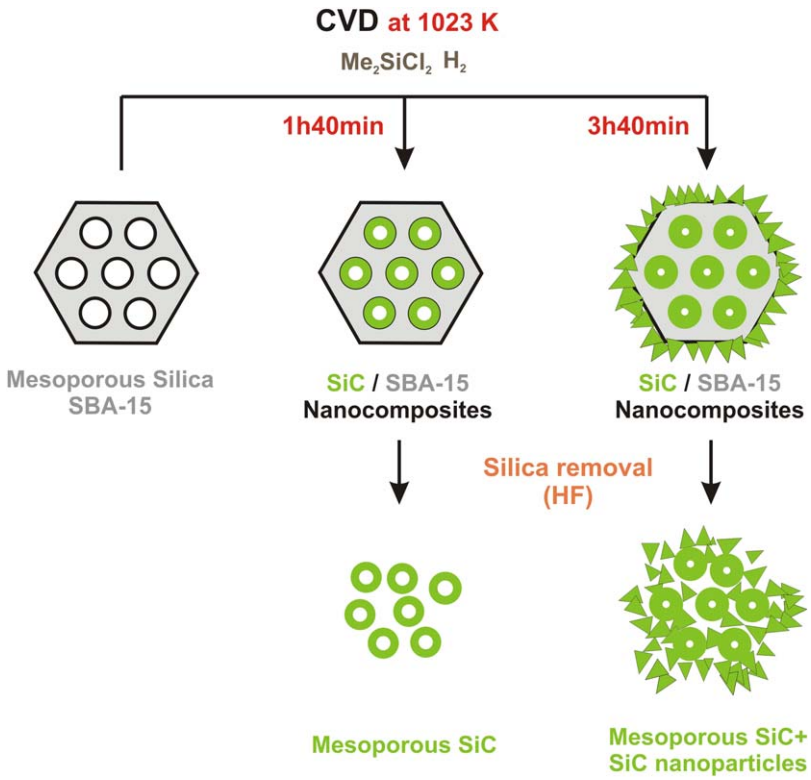

Scheme 1. Chemical vapor infiltration approach for the synthesis of high surface area SiC.

deposition (CVD) and chemical vapor infiltration (CVI) was also used for the impregnation of ordered porous hosts in order to control the size of the deposited domains [20–22]. Silicon carbide can be directly deposited inside MCM-48 and SBA-15 by CVI [23]. CVI allows to use simple and inexpensive precursors and gives good control of the product composition [24].

In the present study the influence of CVI synthesis conditions for SiC/SBA-15 nano-composites on porosity and structure of porous high surface area SiC is discussed. Silicon carbide is obtained by HF treatment of the composite material (Scheme 1). In the following, the high thermal textural stability of mesoporous SiC will be demonstrated and compared to that of other mesoporous materials such as SBA-15 and CMK-1. As a second route, the preparation of SiC from tetramethyl silane (TMS) under high autogenic pressure in the presence of SBA-15 is discussed.

2. Experimental

2.1. SBA-15 synthesis

A somewhat modified procedure of Zhao et al. was used [25]. 4 g Pluronic P123 (BASF) are dissolved in 105 mL of water (500 mL beaker) overnight without stirring. The solution is then heated up to 313 K and 20 mL of 37% HCl (Merck) are added. After 10 min, 8.3 g of TEOS (ACROS 98%) is added dropwise within 30 min and the solution is stirred. The mixture becomes white after few minutes, subsequently the heating is continued for 4 h. The solid is recovered by filtration without washing with water, and the resulting product is immediately calcined at 823 K for 5 h (heating rate 1 K min^{-1}). The as prepared material had a specific surface area of 569 $m^2 g^{-1}$, an average pore diameter of 5.5 nm and a mesopore volume of 0.75 $cm^3 g^{-1}$.

2.2. CVI of DDS into SBA-15

The deposition of SiC on SBA-15 was carried out at atmospheric pressure in a hot-wall vertical quartz tube reactor, 500 mm long and 30 mm in diameter (Supporting Information). The mesoporous host was supported on a quartz frit located in the middle of the tube. Dimethyl dichlorosilane (DDS) (FLUKA 98%) was introduced as the SiC precursor into the reactor from the bottom using a saturator, and hydrogen/argon (4:3) as the gas mixture ($V = 2\,L\,h^{-1}$, DDS evaporation rate $= 1\,mL\,h^{-1}$, $T_{reactor} = 1118\,K$, heating rate $= 10\,K\,min^{-1}$). The host was heated in the carrier gas up to 673 K, and then dimethyl dichlorosilane vapor was introduced. After the specified time at reaction temperature, the reactor was cooled down to room temperature with a cooling rate of 5 K min^{-1}. The prepared composite material was taken out from the reactor and treated with 30% HF solution (200 mL) for 2 days, in order to remove the silica. The resulting porous silicon carbide was washed with water several times and dried at 343 K.

2.3. CVI of TMS into SBA-15

A $\frac{1}{2}$ in swagelok union part was filled with SBA-15 and heated to 523 K under argon for 1 h in order to evaporate physisorbed water. Subsequently TMS—Fluka 99% was added and the vessel was closed (under argon). The closed vessel was placed in a quartz tube and heated to 1273 K in an argon flow with a heating ramp of 120 K h^{-1} and maintained at this temperature for 6 h. Afterwards the resulting SiC/SBA-15 composite was treated with 10% HF solution in order to obtain high surface area SiC.

2.4. CMK-1 synthesis

A procedure reported by Ryoo et al. was used [26]. One gram of MCM-48 was impregnated with a solution of sucrose/H_2SO_4/water (1.25 g/0.077 mL/4.5 g), dried at 343 K for 1 h, at 373 K for 6 h and at 433 K for 6 h. The obtained black solid was ground and impregnated a second time with sucrose solution (0.8 g sucrose/0.049 mL H_2SO_4/3 g water) and heat-treated according to the procedure described above. The pyrolysis was performed at 1173 K for 4 h, with a heating ramp of 60 K h^{-1}. The silica/carbon nano-composite obtained was treated with HF two times, filtered, washed with ethanol and dried at 373 K.

2.5. Thermal stability tests

The sample was placed in a horizontal alumina tube reactor (20 mm diameter and 1000 mm long) in an alumina boat. Before starting the heating program, the tube was purged with argon for 24 h. The furnace was heated to 1573 K with a heating rate of 300 K h^{-1} and maintained at this temperature for the desired time, while the argon flow was maintained at the same level.

2.6. Characterization

Physisorption isotherms were measured at 77 K using a Quantachrome Autosorb-1 apparatus. Prior to the measurement, the samples were evacuated at 353 K for 10 h. High-purity gases were used (nitrogen: 99.999%). The BET surface area was calculated for the relative pressure interval of $P/P_0 = 0.05$–0.3. The mesopore volume was calculated using the BJH theory for pores with diameter in between 2 and 50 nm. X-ray diffraction patterns were recorded in transmission geometry using a STOE Stadi-P diffractometer and Cu $K\alpha_1$ radiation ($\lambda = 0.15405$ nm). Transmission electron micrographs were obtained using a Hitachi HF 2000 TEM using a copper grid-type sample holder. The TG/MS measurements were carried out in air using a Netzsch STA 409PC thermobalance. A heating ramp of 3 K min^{-1} was used.

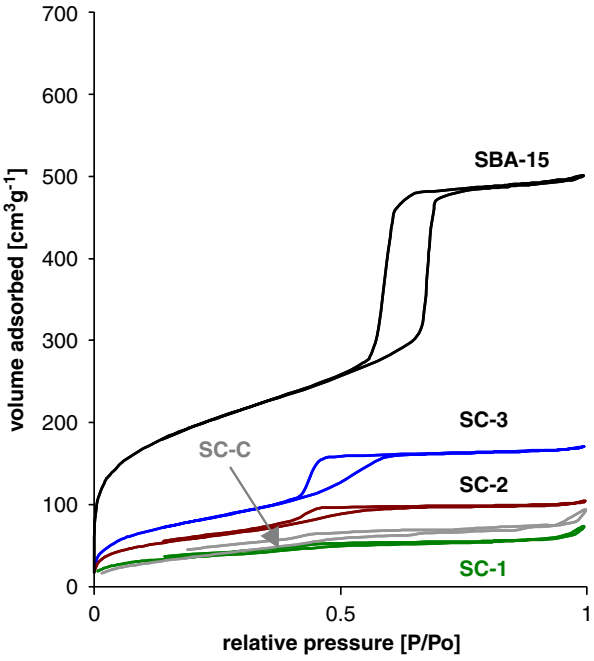

Fig. 1. Nitrogen adsorption isotherms (77 K) of SiC/SBA-15 composite materials.

3. Results and discussion

3.1. Porous SIC—influence of synthesis parameters

The general concepts for the preparation of SiC/SBA-15 nano-composites by CVD were outlined recently [23]. However, only one composite sample was used for the preparation of high surface area mesoporous silicon carbide and the impact of the preparation conditions on the properties of mesoporous SiC was not investigated. In the present study, we describe how the composition of the SiC/SBA-15 composites affects the properties of the mesoporous silicon carbide obtained from them. Three composite samples with different SiC loadings were prepared using different quantities of SBA-15 in the reactor and various durations of infiltration (Fig. 1, Table 1—SC-1,2,3). An additional carbon-rich sample was prepared in argon flow (without hydrogen) (Table 1—SC-C) in order to investigate the influence of carbon impurities on the properties of mesoporous SiC. At 1118 K, DDS decomposes inside the pores of SBA-15 to form SiC (1) (Scheme 1), but when the pore diameter is decreased substantially, deposition of SiC outside the pore system also takes place due to the limited diffusion of precursor molecules into the pore system [23]. In the early stages of deposition significant amounts of silicon oxycarbides are formed on the silica walls, followed by the formation of silicon carbide on top of the silicon oxycarbide layer [23]:

$$(CH_3)_2SiCl_2 \rightarrow SiC + 2HCl + CH_4. \quad (1)$$

After removal of silica from the composite material (Scheme 1), the resulting mesoporous silicon carbide

Table 1
SiC/SBA-15 composites: preparation parameters and characterization

Sample	Infiltration time (h:min)	SBA-15 weight (g)	Weight gain (wt%)	Surface area ($m^2 g^{-1}$)	Average pore diameter[a] (nm)	Mesopore volume[b] ($cm^3 g^{-1}$)
SC-1	3:40	0.6	95	130	3.0	0.06
SC-2	3:40	2	60	213	2.9	0.12
SC-3	1:40	2	30	294	3.5	0.23
SC-C[c]	3:40	0.6	75	140	3.4	0.12

[a]Average pore diameter (d_p) calculated using total pore volume at 0.95 P/P_0 (V_p) and measured specific surface area (S_g) according to equation $d_p = 4V_p/S_g$.
[b]Mesopore volume calculated using the BJH theory for pore size between 2 and 50 nm.
[c]Sample prepared in Ar/DDS flow—without H_2.

Table 2
Mesoporous SiC prepared by HF treatment of SiC/SBA-15 composites

Sample	Composite used	Surface area ($m^2 g^{-1}$)	Average pore diameter[a] (nm)	Mesopore volume[b] ($cm^3 g^{-1}$)	Carbon content (wt%)
SiC-1	SC-1	410	3.1	0.31	25.9
SiC-2	SC-2	578	4.6	0.71	25.2
SiC-3	SC-3	509	7.4	0.96	26.5
SiC-C	SC-C	830	3.1	0.52	36.3

[a]Average pore diameter (d_p) calculated using total pore volume at 0.95 P/P_0 (V_p) and measured specific surface area (S_g) according to equation $d_p = 4V_p/S_g$.
[b]Mesopore volume calculated using the BJH theory for pore size between 2 and 50 nm.

samples had a high specific surface area (higher than that of the SiC/SBA-15 composite material) (Table 2) and showed type IV nitrogen physisorption isotherms, with a broad adsorption step, suggesting a broad pore size distribution (Fig. 2). The overall nitrogen adsorption capacities were increased, as compared to the composite samples and the highest mesopore volume was measured for SiC-3 with $V_g = 0.96\,cm^3 g^{-1}$ and a surface area of $509\,m^2 g^{-1}$. A sample prepared with longer infiltration times (SiC-2) showed significantly lower mesopore volume ($0.71\,cm^3 g^{-1}$), and slightly higher surface area ($578\,m^2 g^{-1}$). On the other hand, SiC-1 prepared from the nano-composite with the highest SiC loading has the lowest surface area and lowest mesopore volume ($410\,m^2 g^{-1}$ and $0.31\,cm^3 g^{-1}$). This clearly indicates that too long infiltration duration and too high loadings lead to deposition of SiC outside the pore structure, resulting in agglomerated materials with larger particles. However, the highest surface area was measured for the carbon-rich sample SiC-C ($830\,m^2 g^{-1}$), while the shape of the isotherm was similar to that of SiC-1 ($410\,m^2 g^{-1}$). The latter is caused by the lower density of carbon materials as compared to the density of silica or silicon carbide. Wide angle X-ray powder diffraction patterns show that mesoporous silicon carbides prepared with short infiltration duration and low loadings (SiC-2, SiC-3) are X-ray amorphous (as well as SiC-C sample), while the sample with the highest loading (SiC-1) is crystalline and reflections of cubic β-SiC (JCPDS: 73-1665) are detected (Fig. 3). On the other hand if the amorphous sample (SiC-2) was heated to 1773 K for

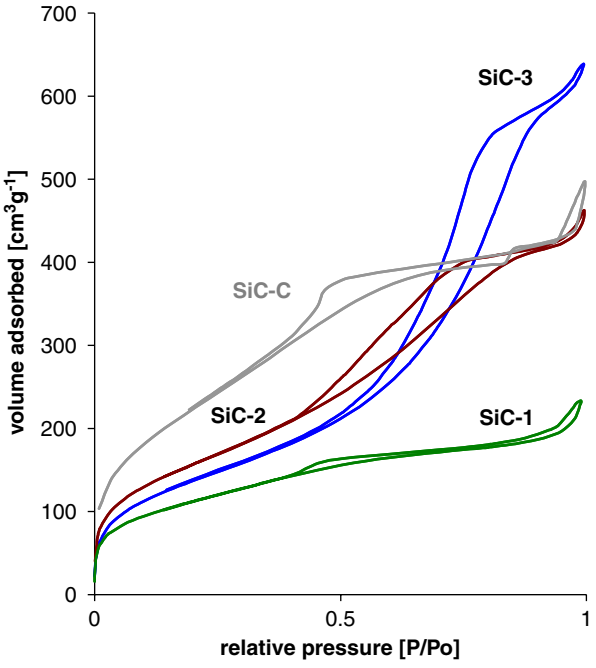

Fig. 2. Nitrogen physisorption isotherms (77 K) of mesoporous SiC samples derived from SiC/SBA-15 composites.

a short time (1 h), β-SiC reflections were also observed (Fig. 3—SiC-3*]. According to ^{29}Si MAS NMR measurements (see Supporting Information) the amorphous materials SiC-1 and SiC-2 were found to be composed mainly of SiC (−8 ppm) [27–29] with a small amount of silicon oxycar-

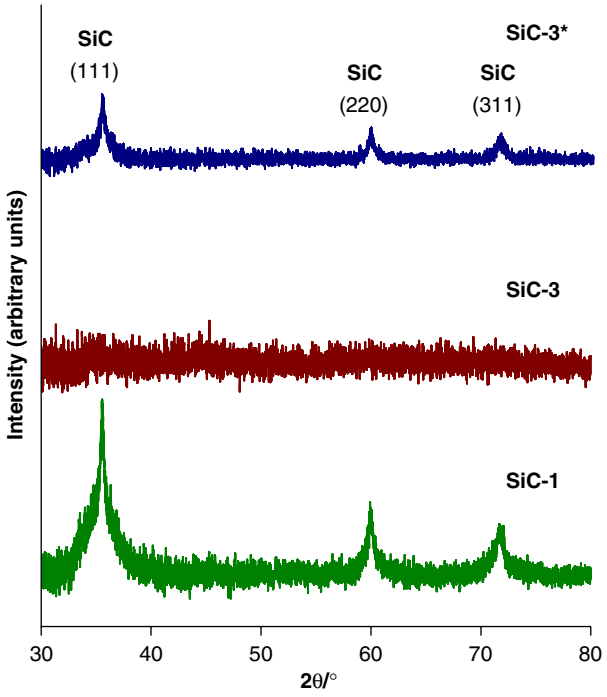

Fig. 3. X-ray diffraction patterns of mesoporous SiC samples. SiC-3* is the SiC-3 sample heat treated in argon at 1773 K for SiC crystallization. SiC-2 and SiC-C were X-ray amorphous.

bide impurities (mainly $SiCO_3$ at −61 ppm, and traces of SiC_2O_2 at −300 ppm and SiC_3O at 15 ppm) [29,30]. The following chemical shifts were used for the assignment of various SiC_xO_y species: SiC: 0 to −16 [27–29], $SiCO_3$: −60 to −71 [29,31], SiC_2O_2: −20 to −38 [29,31], SiC_3O: 5–10 ppm [29,31]. Based on the relative intensities, the lowest amount of oxycarbide species were found for SiC-1 prepared from the composite with the highest weight gain. On the other hand, in SiC-3 the amount of oxycarbides was significantly higher. However, there was no SiO_2 present in any of the measured samples (no peak in the range of −107 to −113 ppm) [31], indicating complete silica removal. The latter is also confirmed in the FT-IR spectra (Fig. 4) with one peak at 819–833 cm^{-1} resulting from Si–C bonds vibration for all samples, as well as smaller contribution of Si–O bonds in between 1034 and 1071 cm^{-1} [32]. The relative intensity of the Si–O peak was highest for SiC-3 in agreement with the NMR data. On the other hand the lowest Si–O peak intensity was observed for the crystalline SiC-1 material. The elemental analysis showed the carbon content in the range of 25–27 wt%, which is slightly lower than the theoretical value of 30 wt% for pure SiC, due to the presence of silicon oxycarbide. However, in case of the SiC–C sample, a higher carbon content (36 wt%) was measured. TG measurements showed a weight gain of 19% at 1573 K in air (SiC-1) due to the surface oxidation of SiC into SiO_2. Although for complete oxidation, 50% weight gain is expected, passivation with silica protects the SiC particles from complete oxidation and process kinetics become significantly slower. In case of the carbon-rich

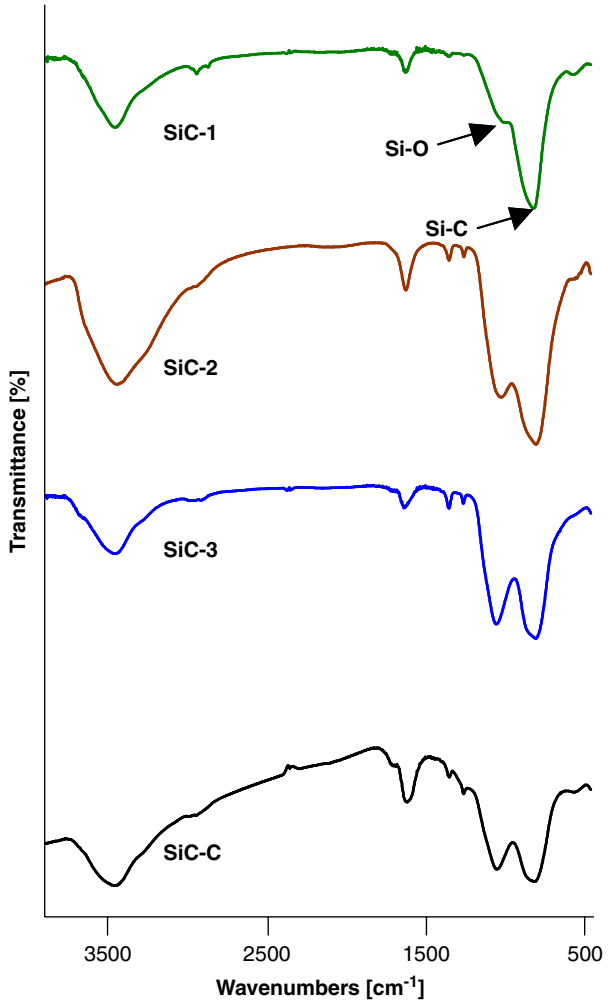

Fig. 4. FT-IR spectra of the mesoporous silicon carbide materials.

SiC–C, a weight loss of 25 wt% was observed due to the burning of the excess free carbon. Transmission electron micrographs of porous SiC-3 (Fig. 5c) reveal a slightly ordered structure (short range ordering) in form of one-dimensional tubes/rods. However, in case of samples prepared with higher matrix loadings (SiC-2 and SiC-1) this rod structure is less visible due to the material deposited outside the pores during the CVI process (Fig. 5a, b). On the other hand, the low angle X-ray measurements do not reveal any long range ordering of all mesoporous SiC samples.

3.2. CVI of TMS into SBA-15

Alternatively to atmospheric pressure deposition of SiC, formation of SiC under high autogenic pressures in the presence of SBA-15 was also studied. The possibility of SiC preparation from simple silanes in an autoclave heated to 1273 K was reported by Pol et al. [19]. However, the surface area of such materials did not exceed 150 $m^2 g^{-1}$. Based on the same principle we used liquid TMS as a precursor and the decomposition was carried out in a closed swagelok cell

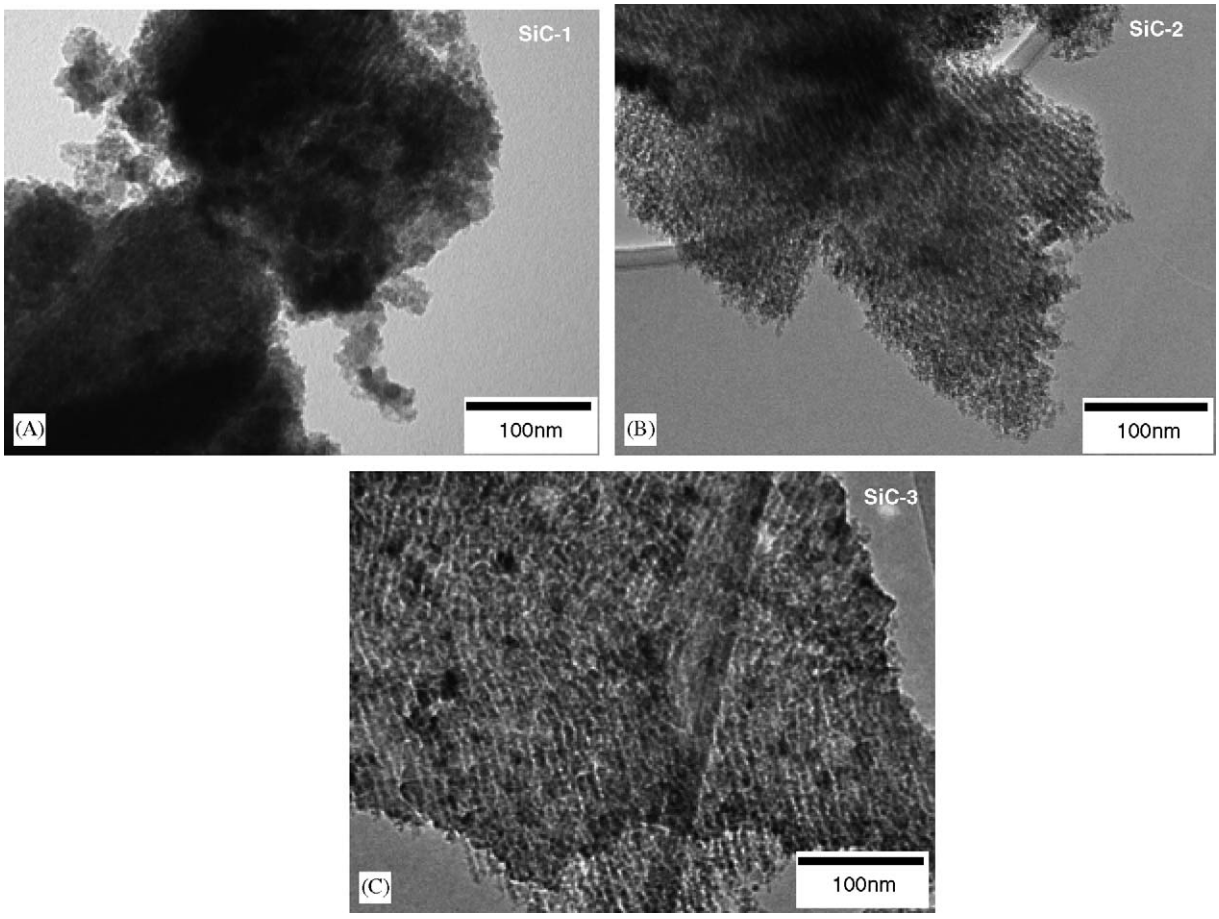

Fig. 5. TEM micrographs of mesoporous SiC samples.

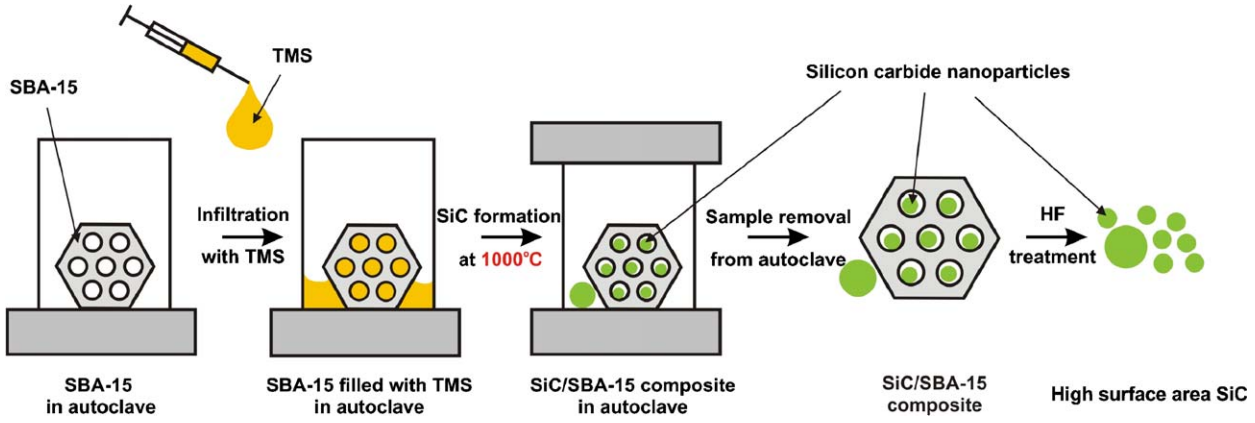

Scheme 2. Preparation of high surface area SiC under autogenic pressure conditions.

in the presence of SBA-15 (Scheme 2). TMS has a high vapor pressure and condenses inside the pores of the mesoporous silica network. Upon the heat treatment to 1273 K it decomposes to form SiC according to reaction (2):

$$Si(CH_3)_4 \rightarrow SiC + 3CH_4. \quad (2)$$

After the synthesis at 1273 K, the autoclave is opened and the resulting product is treated with HF solution in order to dissolve the silica matrix (Scheme 2). For comparison also one sample was prepared without SBA-15 (Table 3—sample AP-SiC*) (only TMS was present in the autoclave). The X-ray powder patterns show the presence of the cubic β-SiC (JCPDS: 73-1665) (Fig. 6) for both samples (AP-SiC: prepared with SBA-15 matrix, and AP-SiC* without SBA-15). In the case of the sample prepared without SBA-15, narrow peaks are observed, indicating the presence of large

Table 3
High surface area SiC prepared under autogenic pressure conditions—parameters of synthesis and textural characteristics

Sample	SBA-15 weight (g)	Volume of TMS added (mL)	Surface area ($m^2 g^{-1}$)	Average pore diameter (nm)	Mesopore volume[a] ($cm^3 g^{-1}$)
[b]AP-SiC*	—	1.50	212	2.3	0.11
[c]AP-SiC-SBA-15	0.225	1.75	387	2.8	0.25
[d]AP-SiC	—	—	636	3.0	0.43

[a]Mesopore volume calculated using the BJH theory for pore size between 2 and 50 nm.
[b]SiC prepared in the absence of SBA-15.
[c]Composite of SiC and SBA-15 before dissolving of the silica matrix.
[d]SiC prepared by HF treatment of SiC/SBA-15 composite material (AP-SiC-SBA-15).

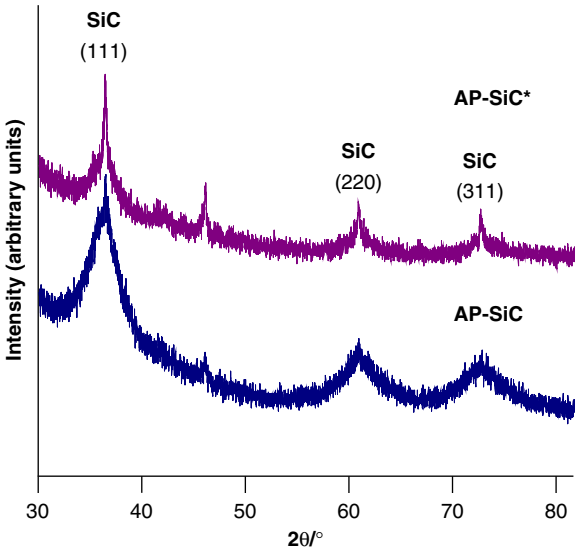

Fig. 6. X-ray diffraction patterns of high surface area silicon carbide synthesized under autogenic pressure with (AP-SiC) or without (AP-SiC*) the presence of ordered mesoporous silica SBA-15.

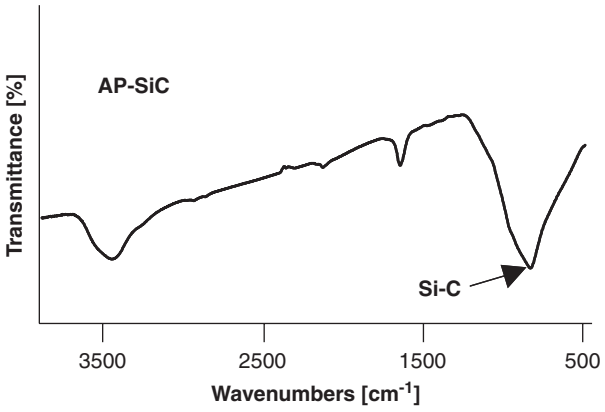

Fig. 7. FT-IR spectrum of AP-SiC.

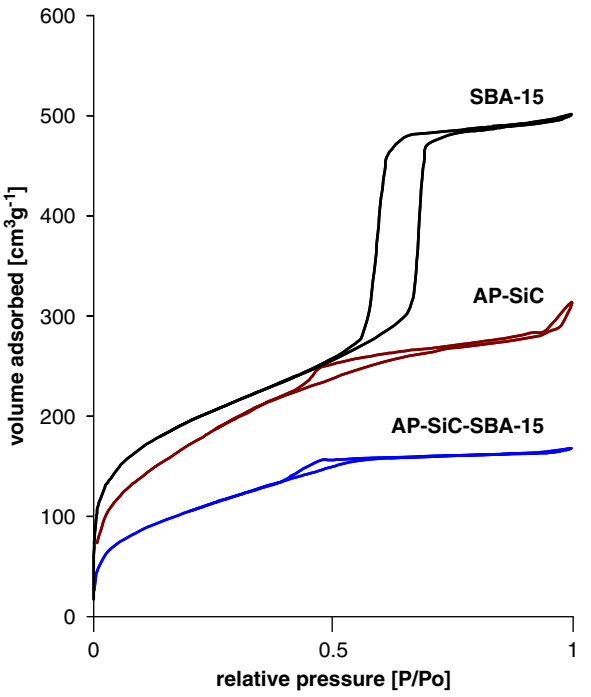

Fig. 8. Nitrogen physisorption isotherms (77 K) of materials prepared via TMS infiltration.

crystallites. On the other hand, the sample prepared in the presence of SBA-15 shows broad peaks, and the crystallite size calculated according to the Scherrer equation was found to be 4 nm. The FT-IR spectra of AP-SiC shows Si–C vibrations at 820 cm^{-1} and the absence of Si–O bonds (Fig. 7). The high specific surface area (636 $m^2 g^{-1}$) confirms that in case of AP-SiC, small nanoparticles were synthesized inside the pores of SBA-15. On the other hand the residual surface area of 387 $m^2 g^{-1}$ measured for the composite material AP-SiC-SBA-15, suggests that the pores of SBA-15 were not filled completely (Table 3). The AP-SiC* material prepared without SBA-15 as a matrix shows significantly lower specific surface area of 212 $m^2 g^{-1}$, which is in a good agreement with the X-ray diffractograms showing narrow peaks due to the presence of larger particles. Nitrogen physisorption isotherms (Fig. 8) show that both, the nanocomposite material and the resulting SiC have a broad range of capillary condensation from $P/P_0 = 0.1$–0.5. The mesopore size distribution is therefore broad (between 2 and 5 nm according to BJH theory) and micropores are present as well. Elemental analysis shows a carbon content of 27 wt% being close to the theoretical value for pure SiC (30%). The latter is also in good agreement with TG measurements showing 28% weight gain due to the oxidation of SiC to SiO_2, the highest

Table 4
Specific surface areas of the mesoporous silicon carbide materials, SBA-15 and CMK-1 after heat treatment at 1573 K

Sample	Original Surface area ($m^2 g^{-1}$)	Original mesopore volume[a] ($cm^3 g^{-1}$)	Surface area after 6 h at 1573 K ($m^2 g^{-1}$)	Mesopore volume[a] after 6 h at 1573 K ($cm^3 g^{-1}$)	Surface area after 24 h at 1573 K ($m^2 g^{-1}$)	Mesopore volume[a] after 24 h at 1573 K ($cm^3 g^{-1}$)
SiC-1	410	0.31	92	0.13	8	<0.05
SiC-2	578	0.71	446	0.48	43	<0.05
SiC-3	509	0.96	291	0.51	145	0.29
SiC-C	830	0.52	354	0.22	5	<0.05
AP-SiC	636	0.43	254	0.19	38	<0.05
SBA-15	569	0.75	<1	—	<1	—
CMK-1	1761	1.05	1637	0.82	1528	0.76

[a]Mesopore volume calculated using the BJH theory for pore size between 2 and 50 nm.

value among all samples, confirming that the small particles only have minor impurities of free carbon. IR measurements confirm the lowest amount of Si–O bonds (silicon oxycarbides) among all the samples.

3.3. Thermal stability of SiC, SBA-15 and CMK-1 at 1573 K

For the investigation of the thermal textural stability, silicon carbide samples were compared with the ordered mesoporous carbon CMK-1 and the pure SBA-15 template. The stability of the latter one was already investigated earlier [33], however, for CMK materials only thermogravimetric data were available [34]. All samples were heated to 1573 K in an inert atmosphere (Argon) for a given duration (Table 4). Ordered mesoporous silica SBA-15 collapses already after 1 h of the heat treatment, showing almost no nitrogen adsorption capacity and the surface area is below $1\,m^2 g^{-1}$ (Table 4). In contrast, mesoporous silicon carbide materials have significantly higher thermal stability in inert conditions (Table 4). In the first 6 h of treatment the specific surface area decreases by 23% for SiC-2 and 78% for SiC-1, while for the 24 h treatment reduction by 63% (SiC-3) and 99% (SiC-C) can be observed. The latter can be an effect of sintering of nano-sized silicon carbide material, as well as of decomposition of oxycarbide species into gaseous products (3) or reaction of SiO_2 with SiC and subsequent formation of SiO and CO:

$$SiO_xC_y \rightarrow SiO + CO, \quad (3)$$

$$SiO_xC_y \rightarrow SiC + SiO_2 \rightarrow SiO + CO. \quad (4)$$

Materials with the lowest amount of silicon oxycarbide (SiC-1, AP-SiC) showed lowest thermal stability and after 6 h of treatment reduction of the surface area by 78% (to $92\,m^2 g^{-1}$) and 60% (to $254\,m^2 g^{-1}$) was observed, respectively. On the other hand these materials have small pore diameters (3.1 and 3.0 nm, respectively). The materials with large pores (SiC-3 and SiC-2) showed better thermal stability. For the SiC-2 sample with an average pore diameter of 4.6 nm (and medium content of oxycarbide species), after 6 h treatment, reduction of surface area by 23% (to $446\,m^2 g^{-1}$) and mesopore volume to $0.48\,cm^3 g^{-1}$ was observed (Fig. 9). A longer treatment resulted in a decrease of surface area to $43\,m^2 g^{-1}$ (reduction by 92%). SiC-3 with the largest pore diameter (7.4 nm) showed the highest textural thermal stability among all silicon carbide samples, and the remaining surface area of $145\,m^2 g^{-1}$ (reduction by 63%) was measured after 24 h treatment. Also a high mesopore volume of $0.29\,cm^3 g^{-1}$ was observed after the long treatment. The thermal stability of SiC-2 was also tested in air at 1573 K, but the surface area decreased to values lower than $1\,m^2 g^{-1}$, already after reaching this temperature. Subsequently, in the X-ray diffractogram narrow reflections of cristobalite were observed (JCPDS:

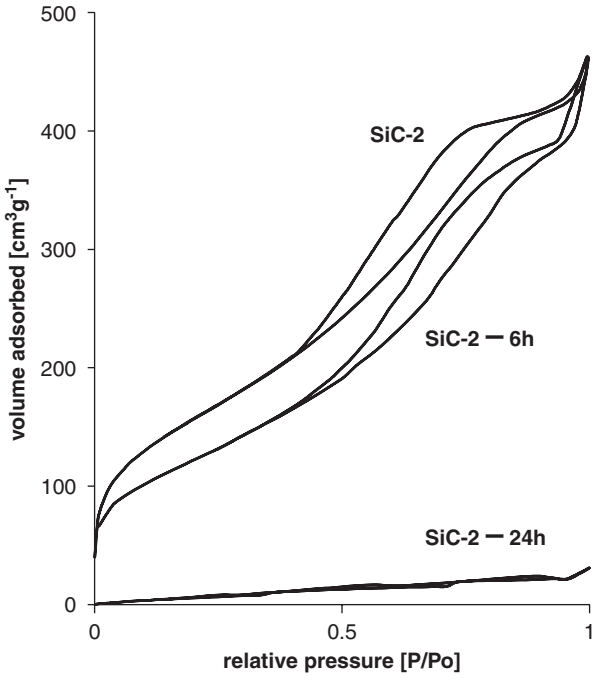

Fig. 9. Nitrogen adsorption isotherms (77 K) of mesoporous SiC-2 heat-treated at 1573 K in argon for 6 and 24 h.

39-1425) for this sample. This suggests a much lower thermal stability under oxidizing conditions at high temperatures due to the oxidation of SiC to SiO_2. On the other hand such a result was to be expected, since SiC is known to form a silica passivation layer under oxidizing conditions at higher temperatures [35]. In case of large micrometer-sized SiC particles such a thin passivation layer protects them from further oxidation, but in case of nanoparticles, SiC can be completely oxidized.

The thermal stability of the ordered mesoporous carbon CMK-1 was found to be even higher than that of silicon carbide. The loss of surface area after 6 h was not significant (from 1761 to 1637 $m^2 g^{-1}$) and the high surface area was observed even after 24 h treatment (1528 $m^2 g^{-1}$). However, low angle X-ray diffractograms show, although a high surface area was retained, already after the short treatment time (6 h), the periodic three-dimensional structure of CMK-1 collapsed and no peaks were detected. The high temperature can cause contraction of the mesoporous matrix (significant reduction of mesopore volume without the reduction of overall sorption capacity at 0.95 P/P_0).

4. Conclusion

We have shown how different precursors, deposition parameters and loadings of SiC/SBA-15 nano-composites influence the textural properties of mesoporous silicon carbide prepared from them. High loadings cause deposition outside of SBA-15 channels and thus, the obtained SiC material has a low surface area and mesopore volume. On the other hand, composites with lowest loading produce SiC materials with a high mesopore volume but a broad pore size distribution and high surface area of 510 $m^2 g^{-1}$. As an alternative route to the ambient pressure CVD process also deposition at high autogenic pressures can be employed resulting in materials with even higher surface area (626 $m^2 g^{-1}$). The elemental analysis indicates the formation of silicon oxycarbide on the surface of high surface area SiC. The amount of free carbon deposited was examined using thermogravimetric measurements in air and elemental analysis, and was found to increase the measured specific surface areas if deposited in excess due to the lower density of porous carbon materials.

High surface area silicon carbide shows a higher thermal stability at 1573 K as compared to pure SBA-15. However, the thermal stability of ordered mesoporous carbon (CMK-1) is even better than that of porous SiC tested under the same conditions.

Appendix A. Supporting information

Supplementary data associated with this article can be found in the online version at doi:10.1016/j.jssc.2006.02.034.

References

[1] K.A. Schwetz, in: R. Riedel (Ed.), Handbook of Ceramic Hard Materials, vol. 1, Wiley-VCH, Weinheim, 2000, pp. 683–740.
[2] M. Raczka, G. Gorny, L. Stobierski, K. Rozniatowski, Mater. Charact. 46 (2001) 245–249.
[3] L. Stobierski, A. Gubernat, Ceram. Int. 29 (2003) 287–292.
[4] I.A. Ibrahim, F.A. Mohamed, E.J. Lavernia, J. Mater. Sci. 26 (1991) 1137–1156.
[5] T.P.D. Rajan, R.M. Pillai, B.C. Pai, J. Mater. Sci. 33 (1998) 3491–3503.
[6] M. Mitomo, Y.W. Kim, H. Hirotsuru, J. Mater. Res. 11 (1996) 1601–1604.
[7] M. Sternitzke, J. Eur. Ceram. Soc. 17 (1997) 1061–1082.
[8] M.J. Ledoux, C. Pham-Huu, Cattech 5 (2001) 226–246.
[9] R. Moene, M. Makkee, J.A. Moulijn, Appl. Catal. A 167 (1998) 321–330.
[10] M.J. Ledoux, S. Hantzer, C.P. Huu, J. Guille, M.P. Desaneaux, J. Catal. 114 (1988) 176–185.
[11] C. Phamhuu, P. Delgallo, E. Peschiera, M.J. Ledoux, Appl. Catal. A 132 (1995) 77–96.
[12] M.B. Kizling, P. Stenius, S. Andersson, A. Frestad, Appl. Catal. B 1 (1992) 149–168.
[13] M.A. Vannice, Y.L. Chao, R.M. Friedman, Appl. Catal. 20 (1986) 91–107.
[14] P.H. Cuong, S. Marin, M.J. Ledoux, M. Weibel, G. Ehret, M. Benaissa, E. Peschiera, J. Guille, Appl. Catal. B 4 (1994) 45–63.
[15] G.Q. Jin, X.Y. Guo, Microporous Mesoporous Mater. 60 (2003) 207–212.
[16] J. Parmentier, J. Patarin, J. Dentzer, C. Vix-Guterl, Ceram. Int. 28 (2002) 1–7.
[17] Z.C. Liu, W.H. Shen, W.B. Bu, H.R. Chen, Z.L. Hua, L.X. Zhang, L. Li, J.L. Shi, S.H. Tan, Microporous Mesoporous Mater. 82 (2005) 137–145.
[18] A.H. Lu, W. Schmidt, W. Kiefer, F. Schüth, J. Mater. Sci. 40 (2005) 5091–5093.
[19] V.G. Pol, S.V. Pol, A. Gedanken, Chem. Mater. 17 (2005) 1797–1802.
[20] C.L. Bowes, A. Malek, G.A. Ozin, Chem. Vapor Depos. 2 (1996) 97–103.
[21] E. Chomski, O. Dag, A. Kuperman, N. Coombs, G.A. Ozin, Chem. Vapor Depos. 2 (1996) 8–13.
[22] O. Dag, G.A. Ozin, H. Yang, C. Reber, G. Bussiere, Adv. Mater. 11 (1999) 474–480.
[23] P. Krawiec, C. Weidenthaler, S. Kaskel, Chem. Mater. 16 (2004) 2869–2880.
[24] I. Golecki, Mater. Sci. Eng. R 20 (1997) 37–124.
[25] D.Y. Zhao, J.L. Feng, Q.S. Huo, N. Melosh, G.H. Fredrickson, B.F. Chmelka, G.D. Stucky, Science 279 (1998) 548–552.
[26] R. Ryoo, S.H. Joo, S. Jun, J. Phys. Chem. B 103 (1999) 7743–7746.
[27] J.R. Guth, W.T. Petuskey, J. Phys. Chem. 91 (1987) 5361–5364.
[28] G. Roewer, U. Herzog, K. Trommer, E. Müller, S. Frühauf, Struct. Bond. 101 (2002) 60–127.
[29] H.M. Williams, E.A. Dawson, P.A. Barnes, B. Rand, R.M.D. Brydson, A.R. Brough, J. Mater. Chem. 12 (2002) 3754–3760.
[30] V. Belot, R.J.P. Corriu, D. Leclercq, P.H. Mutin, A. Vioux, J. Non-Cryst. Solids 144 (1992) 287–297.
[31] Y. ElKortobi, J.B.E. delaCaillerie, A.P. Legrand, X. Armand, N. Herlin, M. Cauchetier, Chem. Mater. 9 (1997) 632–639.
[32] T. Merlemejean, E. Abdelmounim, P. Quintard, J. Mol. Struct. 349 (1995) 105–108.
[33] K. Cassiers, T. Linssen, M. Mathieu, M. Benjelloun, K. Schrijnemakers, P. Van Der Voort, P. Cool, E.F. Vansant, Chem. Mater. 14 (2002) 2317–2324.
[34] M. Kruk, M. Jaroniec, R. Ryoo, S.H. Joo, J. Phys. Chem. B 104 (2000) 7960–7968.
[35] C. Raynaud, J. Non-Cryst. Solids 280 (2001) 1–31.